Journal Name

COMMUNICATION

Investigating the Role of Amine in InP Nanocrystal Synthesis: Destabilizing Cluster Intermediates by Z-Type Ligand Displacement

Received 00th January 20xx,
Accepted 00th January 20xx

DOI: 10.1039/x0xx00000x

www.rsc.org/

Dylan C. Gary, Alessio Petrone, Xiaosong Li, and Brandi M. Cossairt*

The reaction of primary amines with $In_{37}P_{20}(O_2CR)_{51}$ is found to remove $In(O_2CR)_3$ subunits from $In_{37}P_{20}(O_2CR)_{51}$. This loss of Z-type ligands coincides with structural rearrangement to alleviate core strain and passivate phosphorus atoms. This result consolidates conflicting claims that primary amines both promote and retard precursor conversion rates for InP nanocrystals.

Primary amine is a common additive in many nanocrystal syntheses and has been assigned a variety of roles including ligand, shape control agent, proton donor, percursor conversion inhibitor, and growth activator.[1–4] Specifically in the synthesis of indium phosphide quantum dots (InP QDs) from indium carboxylates and silylphosphines, amine has been proposed to play several distinct, and often conflicting roles.[5–7] Xie et al. have suggested that amines act as activating agents for indium carboxylates by increasing their reactivity towards silylphosphines.[5] This hypothesis is consistent with the observation that primary amines lowered the temperature necessary to synthesize InP QDs from silylphosphines and indium carboxylates by about 100 °C. This claim was later refuted by Allen et al. who discovered that amine retards In–P bond formation from silylphosphines and indium carboxylates by monitoring the precursor conversion reactions using NMR spectroscopy.[6] Based on these observations, a reaction mechanism in which amine competes with phosphine for coordination to In prior to In–P bond formation via an S_N2 transition state was proposed.

Xie et al. also demonstrated that InP QDs ranging in size from 2 to 8 nm could be synthesized by altering the concentration of amine and free carboyxlic acid employed in these syntheses. Protière et al. observed in their syntheses that addition of primary amine yielded *in situ* water which would oxidize the surface of the InP QDs, forming an In_2O_3 shell and effectively halting further growth.[7] These apparently contrary observations may be resolved by considering the difference in temperature at which these two studies were carried out. At the lowered temperatures reported by Xie et al. (190 °C rather than 270 °C), the condensation of amine and free carboxylic acid would take place at a slower rate than precursor conversion and growth of InP based upon reported reaction times for the direct amidation of carboxylic acids with primary amines at similar temperatures.[8]

Given that amines have been shown to impede precursor conversion and halt nanocrystal growth at elevated temperatures due to the formation of an In_2O_3 shell, another explanation was needed to account for the observation that the addition of primary amines lowers the temperature necessary to synthesize high quality InP over a large range of sizes. Our group offered an explanation consistent with these observations.[9] We repeated the synthesis of InP reported by Xie et al. at lower temperatures (110–160 °C) in the absence of primary amine. Under these reaction conditions, we obtained a magic-size cluster of InP instead of the larger dynamic structures reported by Xie and coworkers. Addition of primary amine to a solution of these clusters held at 160 °C was shown by UV-Vis absorbance spectroscopy to rapidly induce growth of InP through a continuum of sizes. Therefore, amine can both inhibit precursor conversion in a non-rate limiting step, as well as decrease the temperature necessary for the rate-limiting nucleation of InP nanocrystals from clusters since these are temporally distinct events in a two-step nucleation mechanism. Recently, we have been able to determine the identity of the magic-size cluster in this sythesis to be $In_{37}P_{20}(O_2CR)_{51}$ by single crystal X-ray diffraction.[10] This result has prompted us to further investigate the reaction of primary amine with $In_{37}P_{20}(O_2CR)_{51}$ in order to elucidate its role in destabilizing $In_{37}P_{20}(O_2CR)_{51}$.

Previously, we were able to determine the reaction product of $In_{37}P_{20}(O_2CR)_{51}$ with one equivalent of H_2O in the solid state by exposing single crystals of $In_{37}P_{20}(O_2CCH_2C_6H_5)_{51}$ to moist air for short periods of time. The resultant crystals yielded a new diffraction pattern consistent with a structure in which a single carboxylate ligand had shifted binding modes from bidentate to monodentante and H_2O had datively bound to the available coordination site (Figure 1). This observation suggests that $In_{37}P_{20}(O_2CR)_{51}$ may have site

Department of Chemistry, University of Washington, Box 351700, Seattle, WA 98195-1700. Email: cossairt@chem.washington.edu

† Electronic Supplementary Information (ESI) available: Complete experimental details and additional experimental and computational data and analysis. Crystallographic data can be found under CCDC deposition number 1507652. See DOI: 10.1039/x0xx00000x

selective reactivity towards Lewis bases, and that the indium centre to which water was bound (In16 and its symmetry equivalent In27) is the most likely candidate for initial binding site of primary amines.

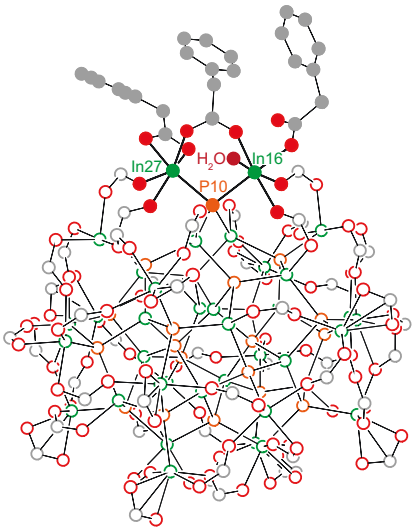

Figure 1. Truncated structure of $In_{37}P_{20}(O_2CCH_2C_6H_5)_{51}{\cdot}H_2O$. Prior to hydration, both In atoms (In16 and In27) bound to P10 exhibited the same first coordination sphere and were related by pseudo C_2 symmetry. Post hydration, one phenylacetate ligand on In16 adopted a monodentate binding mode to accommodate H_2O.

Our first insight into the reaction scheme between primary amines and $In_{37}P_{20}(O_2CR)_{51}$ was obtained by adding 108 equivalents of benzylamine to $In_{37}P_{20}(O_2CCH_2C_6H_5)_{51}$. From this solution, crystals of $In(O_2CH_2C_5H_6)_3(H_2NCH_2C_6H_5)_3$ were obtained (Figure S1). In this structure, indium exhibits an octahedral geometry in which each of the three datively bound benzylamine ligands are trans to a phenylacetate ligand. The liberation of $In(O_2CR)_3$ in an amine-bound form from the surface of $In_{37}P_{20}(O_2CR)_{51}$ is consistent with recent literature illustrating L-type promoted Z-type ligand exchange as a viable strategy for removing anionic carboxylate from QD surfaces using neutral amine.[11]

In light of this discovery, we decided to explore this reaction further by performing a titration of $In_{37}P_{20}(O_2CCH_2C_6H_5)_{51}$ with 1, 3, 6, 12, 24, 48, 100, and 200 equivalents of 4-fluorobenzylamine ($H_2NCH_2C_6H_4F$). We chose 4-fluorobenzylamine in order to specifically probe the fate of the amine additive using $^{19}F\{^1H\}$ NMR spectroscopy. From the $^{31}P\{^1H\}$ NMR data, we see evidence for a stoichiometric reaction upon addition of 1 to 3 equivalents of $H_2NCH_2C_6H_4F$ with complete conversion to a single new product that preserves the pseudo C2 symmetry as evidenced by shifts in all the major resonances associated with $In_{37}P_{20}(O_2CCH_2C_6H_5)_{51}$ (Figure 2A). Based on our assignment of the $^{31}P\{^1H\}$ NMR spectrum for $In_{37}P_{20}(O_2CCH_2C_6H_5)_{51}$ (Figure S2-S6, Tables S1-S3), we observed that upon addition of the first three equivalents of $H_2NCH_2C_6H_4F$ the largest shift in the spectrum is for the phosphorus atom P10 (from –185 ppm to –173 ppm). This interpretation is consistent with our previous assignment of the most acidic site on the cluster residing on In16, which is bound to P10.[10] Between the addition of six and twelve equivalents of $H_2NCH_2C_6H_4F$, we observe that all major resonances have shifted and broadened in the $^{31}P\{^1H\}$ NMR spectrum. This is likely due to the removal of $In(O_2CH_2C_6H_5)_3$ in the form of $In(O_2CCH_2C_6H_5)_3(H_2NCH_2C_6H_5)_3$ with a concurrent structural rearrangement.

$^{19}F\{^1H\}$ NMR spectra were taken of the same solution of $In_{37}P_{20}(O_2CCH_2C_6H_5)_{51}$ with 17 equivalents of α,α,α-trifluorotoluene ($C_6H_4CF_3$) as an internal standard (Figure 2B). All of the ^{19}F nuclei are accounted for throughout these additions within experimental error according to the relative integration of $H_2NCH_2C_6H_4F$ to $C_6H_4CF_3$. Upon addition of a single equivalent of $H_2NCH_2C_6H_4F$ to $In_{37}P_{20}(O_2CCH_2C_6H_5)_{51}$, three major resonances were observed in the $^{19}F\{^1H\}$ spectrum at –114.3 ppm, –115.1 ppm, and –115.3 ppm. We attribute these peaks to $H_2NCH_2C_6H_4F$ tightly binding to the surface of the $In_{37}P_{20}(O_2CCH_2C_6H_5)_{51}$. This initial reaction went to completion in terms of the consumption of $H_2NCH_2C_6H_4F$ since we observed no free $H_2NCH_2C_6H_4F$ (singlet at –118.3 ppm). Up to the addition of 6 equivalents of $H_2NCH_2C_6H_4F$, the $^{19}F\{^1H\}$ spectra can be explained in terms of $H_2NCH_2C_6H_4F$ exhibiting three predominant coordination modes to the surface of $In_{37}P_{20}(O_2CCH_2C_6H_5)_{51}$. Given that each of the ^{31}P nuclei in the $^{31}P\{^1H\}$ NMR spectra could be accounted for with a single structure, but we observed multiple peaks in the $^{19}F\{^1H\}$ spectra from the addition of 1 to 3 equivalents of $H_2NCH_2C_6H_4F$, there may be multiple modes by which $H_2NCH_2C_6H_4F$ can bind to the surface of $In_{37}P_{20}(O_2CCH_2C_6H_5)_{51}$ while preserving a constant phosphide sublattice.

After 12 equivalents of $H_2NCH_2C_6H_4F$ were added to the solution, all of the peaks assigned to the initial binding modes of $H_2NCH_2C_6H_4F$ were lost and a broad singlet grew in around –115.5 ppm. We interpret this to amine having liberated surface bound indium from $In_{37}P_{20}(O_2CCH_2C_6H_5)_{51}$ in the form of $In(O_2CCH_2C_6H_5)_3(H_2NCH_2C_6H_5)_3$. This is consistent with our interpretation of the $^{31}P\{^1H\}$ NMR spectra. Upon further additions of $H_2NCH_2C_6H_4F$, the broad peak attributed to liberated $In(O_2CCH_2C_6H_5)_3(H_2NCH_2C_6H_5)_3$ continued to grow in, sharpen, and shift upfield toward free $H_2NCH_2C_6H_4F$. Since we observe a single broad peak in the ^{19}F NMR spectra after this point, we attributed this resonance to $H_2NCH_2C_6H_4F$ being in equilibrium between datively binding to indium at the surface of the cluster or to $In(O_2CCH_2C_6H_5)_3(H_2NCH_2C_6H_5)_3$ and freely diffusing in solution.

The ^1H NMR spectra of the titration of $In_{37}P_{20}(O_2CCH_2C_6H_5)_{51}$ with $H_2NCH_2C_6H_4F$ exhibited line sharpening over the course of the titration in both the alkyl and aromatic regions of the spectrum (Figure 2C). We have previously shown that the ^1H NMR spectrum of $In_{37}P_{20}(O_2CCH_2C_6H_5)_{51}$ exhibits a large number of peaks from about 2.5 to 4.0 ppm.[10] We assigned these peaks to distinct methylene protons on the ligand set due to hindered rotation about the C–C bond of the carbonyl and methylene carbons based on the ^1H–^1H COSY spectrum. Upon addition of 12 equivalents of $H_2NCH_2C_6H_4F$, we observed that the array of peaks spanning from about 2.5 to 4.0 ppm for the methylene protons of $In_{37}P_{20}(O_2CCH_2C_6H_5)_{51}$ were lost and two broad peaks grew in around 3.5 and 3.4 ppm. This suggests that upon removal of $In(O_2CCH_2C_6H_5)_3$ from $In_{37}P_{20}(O_2CCH_2C_6H_5)_{51}$, the resultant cluster is no longer so densely ligated as to prevent

rotation about the C–C bond of the carbonyl carbon and methylene carbon of the carboxylate ligands. Once again, the point in the titration assigned to the removal of $In(O_2CCH_2C_6H_5)_3$ is consistent with the previous assignments for the $^{19}F\{^1H\}$ and $^{31}P\{^1H\}$ spectra.

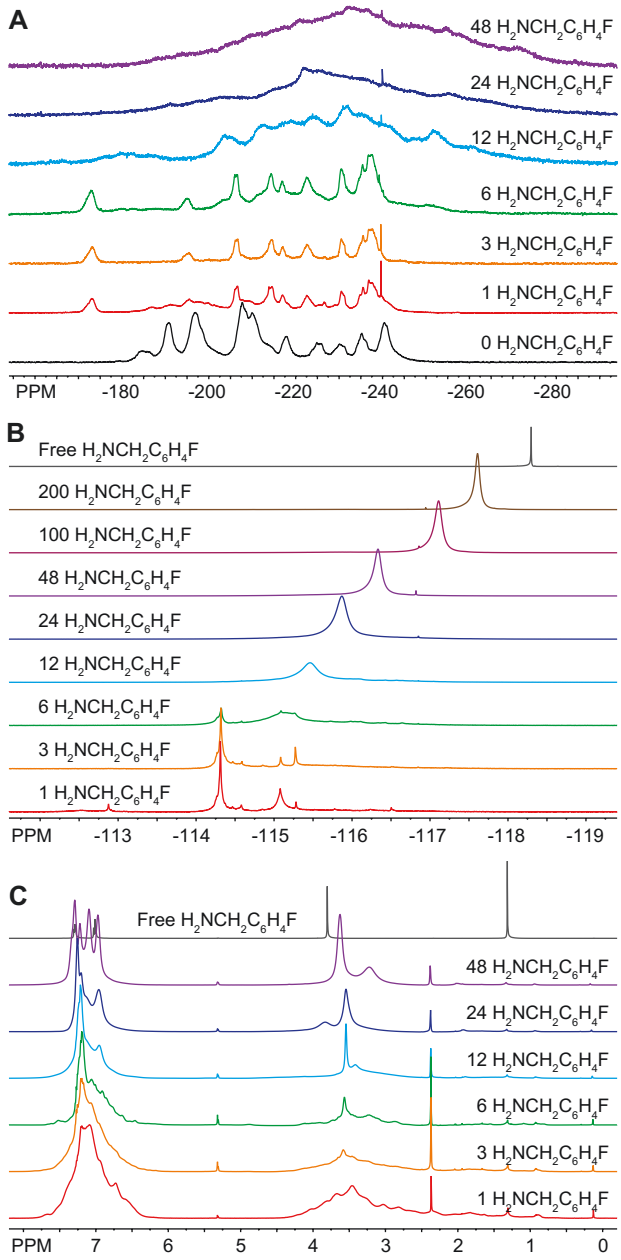

Figure 2. (**A**) $^{31}P\{^1H\}$ (202.3 MHz), (**B**) $^{19}F\{^1H\}$ (469 MHz), and (**C**) ^1H (500 MHz) NMR spectra of $In_{37}P_{20}(O_2CCH_2C_6H_5)_{51}$ after stoichiometric additions of $H_2NCH_2C_6H_4F$ to a solution in CD_2Cl_2.

UV-Vis spectra were also acquired from a titration of $In_{37}P_{20}(O_2CCH_2C_6H_5)_{51}$ with $H_2NCH_2C_6H_4F$ carried out under inert atmosphere (Figure 3). In contrast to the $^{31}P\{^1H\}$, $^{19}F\{^1H\}$, and ^1H NMR spectra, the UV-Vis absorbance spectra of the titration exhibited a continuous shift in which the absorption maximum at 386 nm was lost after a single equivalent of $H_2NCH_2C_6H_4F$ had been added, and a new broad peak at 404 nm gradually grew in up to the addition of 96 equivalents of $H_2NCH_2C_6H_4F$. No further shift in the absorbance maximum at 404 nm was observed in the UV-Vis spectra after the addition of 6 equivalents of $H_2NCH_2C_6H_4F$, even though removal of $In(O_2CCH_2C_6H_5)_3(H_2NCH_2C_6H_5)_3$ is inferred from the NMR at this point in the titration. Analysis of difference spectra (Figure S7) for each sequential data set shows that the major changes in electronic structure are complete following the addition of 12 equivalents of $H_2NCH_2C_6H_4F$, consistent with the structural rearrangement and stabilization of the structure after liberation of $In(O_2CR)_3$.

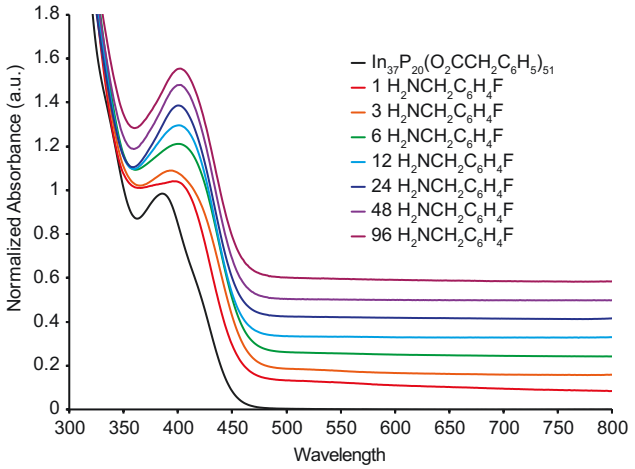

Figure 3. UV-Vis spectra of stoichiometric additions of $H_2NCH_2C_6H_4F$ to a solution of $In_{37}P_{20}(O_2CCH_2C_6H_5)_{51}$ carried out under inert atmosphere. Spectra are normalized to the lowest energy peak maximum and offset vertically for clarity.

Previously, we had predicted that introduction of an indium open coordination site on $In_{37}P_{20}(O_2CCH_2C_6H_5)_{51}$ would be readily identified by UV-Vis spectroscopy.[10] This hypothesis was based on DFT calculations performed on the structure of $In_{37}P_{20}(O_2CCH_2C_6H_5)_{51}{\cdot}H_2O$ and a theoretical structure where H_2O was omitted but the displaced carboxylate ligand remained monodentate, leaving an open coordination site on In16. In order to ascertain whether under-coordinated phosphorus atoms (which must be introduced when breaking the In–P bond to liberate $In(O_2CR)_3$) would have a similar effect, we performed DFT calculations. These calculations show that the UV-Vis spectrum is strongly affected when an open coordination site is present by removing In16 with three carboxylate ligands from $In_{37}P_{20}(O_2CCH_2C_6H_5)_{51}$ (Figure S8). We then mimicked the structural rearrangement by performing geometry optimizations on structures where the phenyl moieties were replaced by acetate, $In_{36}P_{20}(O_2CCH_3)_{48}$. In this case, by allowing the system to relax when In16 was removed along with three carboxylate ligands, a significant change in the electronic properties is still observed (Figure S9 and S10). These calculations suggest that under-coordinated phosphorus atoms would also be readily identified by UV-Vis spectroscopy.

Since we observe no clear evidence for a new species in the UV-Vis spectra between the addition of 6 and 12 equivalents where we propose the loss of $In(O_2CCH_2C_6H_5)_3$ from analysis of the NMR spectra, we hypothesize that upon removal of $In(O_2CCH_2C_6H_5)_3$ from $In_{37}P_{20}(O_2CCH_2C_6H_5)_{51}$ a structural rearrangement occurs in order to

both alleviate core strain and fully passivate all phosphorus atoms. Powder X-ray diffraction data is consistent with such a structural rearrangement with shift in the major reflections to larger angles, potentially indicating a release of compressive strain in the crystallites (Figure S11). Such correlations between surface chemistry and lattice strain have been previously proposed for CdSe and CdS quantum belts.[12] If this hypothesis is valid, it serves to highlight the complementary information available from NMR and UV-Vis spectroscopy for $In_{37}P_{20}(O_2CCH_2C_6H_5)_{51}$.

We hypothesize that the number of atoms removed from the surface of each cluster is two by the following logic. At least 6 equivalents of amine are necessary to remove two indium atoms in the form of $In(O_2CH_2C_5H_6)_3(H_2NCH_2C_6H_5)_3$, and 12 equivalents are necessary to remove 4 indium atoms. Liberation of $In(O_2CH_2C_5H_6)_3(H_2NCH_2C_6H_5)_3$ was implicated between the addition 6 and 12 equivalents of $H_2NCH_2C_6H_4F$. Taken together, this restricts the number of $In(O_2CH_2C_5H_6)_3(H_2NCH_2C_6H_4F)_3$ molecules liberated to at most 4. Adding free carboxylic acid to amine treated clusters suggested that a fraction of the added amine remains datively bound to the surface of the cluster after removal of $In(O_2CH_2C_5H_6)_3(H_2NCH_2C_6H_4F)_3$, which would not leave enough amine to account for the removal of four indium atoms (Figure S12). In16 is the most likely candidate for removal and is chemically indistinguishable from In27 prior to addition of amine. If amine is capable of removing In16, it is likely that In27 would also be removed upon further addition of amine. The removal of three indium atoms from the cluster surface would leave an insufficient number available to fully passivate 20 phosphorus atoms in a tetrahedral environment, and therefore at most two indium atoms are proposed to be removed prior to rearrangement.

$In_{37}P_{20}(O_2CCH_2C_6H_5)_{51}$ has a metal to pnictogen ratio that is similar to the metal to chalcogen ratio of $Cd_{35}Se_{20}$, a known magic-size cluster of CdSe.[13] The structure of $Cd_{35}Se_{20}$ is a zincblende, metal-rich tetrahedron in which each Se is tetrahedrally coordinated to four Cd atoms. Given that 35 indium atoms are necessary to passivate an indium-rich, zincblende regular tetrahedron of InP with 20 phosphorus atoms and we observe no phosphorus dangling bonds in the final product by UV-Vis spectroscopy, we propose a reaction scheme between $In_{37}P_{20}(O_2CR)_{51}$ and H_2NR' in which two equivalents of $In(O_2CR)_3(H_2NCR')_3$ are removed from $In_{37}P_{20}(O_2CR)_{51}$ to yield a regular tetrahedron (or a structure that is symmetrically intermediate between the C_2 and T_d limits) with the formula $In_{35}P_{20}(O_2CR)_{45}$ (Scheme 1). Given the broadness of the solution $^{31}P\{^1H\}$ NMR data and the broadening we observe in the powder X-ray diffraction data, it seems likely that the structure might be dynamic with multiple structures present as an equilibrium mixture.

In conclusion, we have explored the reaction of $In_{37}P_{20}(O_2CR)_{51}$ with primary amines via $^{31}P\{^1H\}$, $^{19}F\{^1H\}$, and ^1H NMR and UV-Vis spectroscopy. We have determined that addition of up to three equivalents of primary amine results in strong binding of amine to specific indium centres by $^{31}P\{^1H\}$, $^{19}F\{^1H\}$, and ^1H NMR spectroscopy. Removal of fewer than four indium atoms is inferred from the abrupt changes observed in the NMR spectra between 6 and 12 equivalents of amine and the isolation of $In(O_2CCH_2C_6H_5)_3$ as a tris(amine) complex from the reaction mixture. Evolution of the inorganic core structure was observed by the $^{31}P\{^1H\}$ NMR spectroscopy following displacement of In^{3+}. A decrease in ligand density as implicated by the loss of hindered rotation about the methylene and carbonyl carbon atoms in the ligand set was also observed by ^1H NMR spectroscopy. These changes were not reflected in the UV-Vis spectroscopy which may be more sensitive to the surface chemistry, especially the presence of under-coordinated indium or phosphorus atoms.

We have proposed a reaction scheme in line with these observations in which removal of two equivalents of $In(O_2CR)_3$ from $In_{37}P_{20}(O_2CR)_{51}$ allows for structural rearrangement to a regular tetrahedron (or a structure of intermediate symmetry) with the formula $In_{35}P_{20}(O_2CR)_{45}$. The irregular structure observed for the magic-size cluster of InP in the absence of L-type ligands ($In_{37}P_{20}(O_2CR)_{51}$) may be due to the preference to fully passivate surface bound indium atoms while simultaneously meeting the demands of charge-balance leading to a dense, interconnected ligand network that distorts the preferred bulk geometry of InP. This would also explain the quasi spherical shape of $In_{37}P_{20}(O_2CR)_{51}$ since this geometry would minimize surface area and thereby maximize the opportunity for bridging-binding modes to fully passivate surface bound indium atoms.

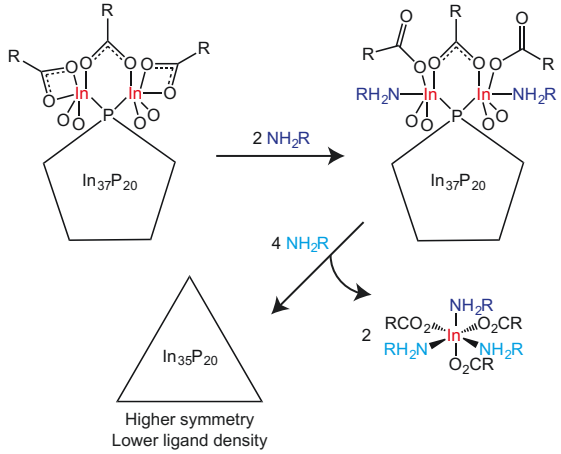

Scheme 1 Proposed reaction scheme between $In_{37}P_{20}(O_2CR)_{51}$ and primary amine. It is likely that primary amine binds dynamically with the surface of the final clusters.

This material is based upon work supported by the National Science Foundation under Grant Numbers CHE- 1552164 (BMC and DCG – synthesis and characterization), CHE-1565520 and DMR-1408617 (AP, XL – DFT calculations). This work was facilitated through the use of advanced computational, storage, and networking infrastructure provided by the Hyak supercomputer system at UW, funded by the Student Technology Fee. We thank Jennifer Stein and Max Friedfeld for acquiring the powder X-ray diffraction data.

References

1 R. García-Rodríguez and H. Liu, *J. Am. Chem. Soc.*, 2014, **136**, 1968–1975.

2 H. You, X. Liu, H. Liu and J. Fang, *Cryst. Eng. Comm.*, 2016, **18**, 3934–3941.

3 K. Yu, X. Liu, Q. Y. Chen, H. Yang, M. Yang, X. Wang, X. Wang, H. Cao, D. M. Whitfield, C. Hu and Y. Tao, *Angew. Chem. Int. Ed.*, 2014, **53**, 6898–6904.
4 K. Kim, D. Yoo, H. Choi, S. Tamang, J.-H. Ko, S. Kim, Y.-H. Kim and S. Jeong, *Angew. Chem. Int. Ed.*, 2016, **55**, 3714–3718.
5 R. Xie, D. Battaglia and X. Peng, *J. Am. Chem. Soc.*, 2007, **129**, 15432–15433.
6 P. M. Allen, B. J. Walker and M. G. Bawendi, *Angew. Chem. Int. Ed.*, 2010, **49**, 760–762.
7 M. Protiere and P. Reiss, *Chem. Commun.*, 2007, 2417–2419.
8 L. J. Gooßen, D. M. Ohlmann and P. P. Lange, *Synthesis*, 2008, **2009**, 160–164.
9 D. C. Gary, M. W. Terban, S. J. L. Billinge and B. M. Cossairt, *Chem. Mater.*, 2015, **27**, 1432–1441.
10 D. C. Gary, S. E. Flowers, W. Kaminsky, A. Petrone, X. Li and B. M. Cossairt, *J. Am. Chem. Soc.*, 2016, **138**, 1510–1513.
11 N. C. Anderson, M. P. Hendricks, J. J. Choi and J. S. Owen, *J. Am. Chem. Soc.*, 2013, **135**, 18536–18548.
12 Y. Zhou, F. Wang and W. E. Buhro, *J. Am. Chem. Soc.*, 2015, **137**, 15198–15208.
13 A. N. Beecher, X. Yang, J. H. Palmer, A. L. LaGrassa, P. Juhas, S. J. L. Billinge and J. S. Owen, *J. Am. Chem. Soc.*, 2014, **136**, 10645–10653.